Synthesis of Sustainable Dual-Function Aerogels from Water Hyacinth Cellulose and Shrimp Shell Nano-Chitosan for Heavy Metal Removal and Coliform Bacteria Filtration in Polluted Water

Saddam Al Husain[1], *Lava* Febrian[2], *Muhammad* Ismail[3], *Siti* Anjani Putri[1], *Muhammad Fauzan* Al Baihaqi[4], *Wahyu* Ramadhan[1,5,*]

[1]Department of Aquatic Product Technology, Faculty of Fisheries and Marine Sciences, IPB University, Bogor, West Java, 16680, Indonesia
[2]Department of Biochemistry, Faculty of Mathematics and Natural Science, IPB University, Bogor, West Java, 16680, Indonesia
[3]Department of Chemistry, Faculty of Mathematics and Natural Science, IPB University, Bogor, West Java, 16680, Indonesia
[4]Department of Agricultural Industrial Engineering, Faculty of Agricultural Engineering and Technology, IPB University, Bogor, West Java, 16680, Indonesia
[5]Center for Coastal and Marine Resources Studies (PKSPL), International Research Institute for Maritime, Ocean and Fisheries (i-MAR), IPB University, 16127, Bogor, Indonesia

Abstract. Rivers are essential water sources but are increasingly polluted by urban waste containing heavy metals and harmful bacteria. An effective solution is optimizing an eco-friendly water hyacinth cellulose aerogel and shrimp shell nano-chitosan for heavy metal adsorption and coliform bacteria filtration. This study extracted cellulose from water hyacinth (S-EG) and chitosan from shrimp shells, followed by nano-chitosan synthesis and aerogel formulation with three cellulose-to-nano-chitosan ratios: F1 (2:1), F2 (1:1), and F3 (1:2). Gel precursors were characterized, and adsorption and filtration capacities were tested to identify the optimal formula. Results showed yields of 12.46% for S-EG, 11.23% for chitosan, and 80% for nano-chitosan. Among the formulas, F3 had the best properties, including 80.16% gel content, 143.41% swelling ratio, and 3630 cPs viscosity. The F3 aerogel achieved 97% porosity, a surface area of 243.5 m^2/g, and a low density of 0.07 g/cm^3. Adsorption capacities were significant, reaching 99.5% for Cu, 88.68% for Zn, and 7.33% for Pb, along with a 30% reduction in *E. coli*. These findings indicate that the 1:2 cellulose-to-nano-chitosan aerogel formulation is highly promising as a sustainable solution for heavy metal adsorption and bacterial filtration in polluted water systems.

* Corresponding author: wahyu.ramadhan@apps.ipb.ac.id

1 Introduction

Water resources are critical for sustaining human life. As global population growth accelerates, the demand for clean water continues to rise. These water resources are primarily derived from rainwater, surface water (such as rivers, lakes, and channels), and groundwater. However, the exploitation of groundwater is constrained due to its potential to destabilize land surfaces when over extracted. Consequently, surface water, which flows through rivers or is stored in lakes and reservoirs, provides the most abundant source and is utilized for various purposes, including potable water, industrial applications, and household use. The volume of surface water is estimated at approximately 0.35 million km^3, constituting only 1% of the Earth's freshwater reserves [1]. In Indonesia, the demand for clean water continues to escalate with population growth. In 2022, the country produced 5,267 million meter cubic of clean water, with allocations of 98.5 million meter cubic for daily needs, 457.9 million meter cubic for commerce and industry, 2,998.5 million meter cubic for non-commercial uses, and 161.2 million meter cubic for other applications [2].

The production of clean water involves several stages, including coagulation, flocculation, sedimentation, filtration, and disinfection [3]. Among these, the filtration stage plays a crucial role in removing particles that remain suspended after sedimentation. However, river water is frequently contaminated by agricultural runoff, industrial effluents, and domestic waste, necessitating preliminary treatment processes to eliminate the pollutants [4]. This contamination is largely attributed to the insufficient availability of water treatment infrastructure, which results in waste entering rivers in volumes that exceed their natural capacity to cope with pollution [5]. Heavy metal and coliform contamination can be mitigated through various methods, including remediation, adsorption, ion exchange, and membrane separation. Among these, adsorption is widely employed in industrial applications due to its cost-effectiveness and non-toxic nature [6]. Aerogels have emerged as promising adsorbent materials for environmental remediation. These porous materials are characterized by their lightweight structure, excellent absorption capacity, large surface area, and high porosity [7]. Commonly used adsorbents, such as zeolites and activated carbon, have proven effective [8]. However, there is a growing need to develop and optimize biopolymer-based aerogels for enhanced performance.

Biopolymers such as cellulose and chitosan are promising materials for aerogel production due to their biodegradability and biocompatibility [9]. One notable source of cellulose is water hyacinth, which contains 64.51% cellulose [10]. The proliferation of water hyacinth has contributed to eutrophication in the Jatiluhur Reservoir, covering approximately 10% of the reservoir's surface area [11]. Chitosan, on the other hand, can be derived from shrimp shells, with a chitosan content of 12.46% [12]. The availability of shrimp shells in Indonesia is substantial, with shrimp production reaching 87,135 tons per year [13]. This high shrimp production makes shrimp a potential source for producing chitosan. Chitosan exhibits notable antimicrobial properties and the capacity for heavy metal adsorption [14]. When synthesized in nanoparticle form (100–400 nm), chitosan demonstrates enhanced efficacy in both bacterial inhibition and heavy metal adsorption [15]. However, due to its low mechanical strength, chitosan requires reinforcement from another polymer, such as cellulose, which can improve structural integrity through the formation of a 3D interconnected network [16]. Consequently, the combination of cellulose and nano-chitosan offers a promising approach for the development of aerogels with dual functions. This study aims to identify the optimal aerogel formulation using cellulose derived from water hyacinth and nano-chitosan from shrimp shells, with the goal of achieving high performance in heavy metal adsorption and bacterial filtration while maintaining environmental sustainability.

2 Materials and Methods

2.1 Materials

The materials used in this research are water hyacinth from the waters of Cibanteng Swamp, Bogor Regency and shrimp shells from seafood restaurants in Muara Angke, North Jakarta, heavy metals (Zn, Pb, Cu) (Merck), *Escherichia coli* (Biology Department, Bogor) nutrient agar (NA) (Merck), nutrient broth (NB) (Merck), eosin methylene blue agar (EMBA) (Merck), sodium alginate (CV. Kimia Jaya Labor, Cirebon) sodium tripolyphosphate (STPP) (CV. Kimia Jagat, Bogor), ethanol (Merck), H_2O_2 (CV. Kimia Jagat, Bogor), NaOH (CV.Kimia Jagat, Bogor), HCl (CV. Kimia Jagat, Bogor), HNO_3 (CV. Kimia Jagat, Bogor), $CaCl_2$ (CV. Kimia Jagat, Bogor), Tween 80 (CV. Kimia Jagat, Bogor), and urea (Merck). The tools used were dehydrator, freeze dryer (Lyovapor L200, Bogor), ImageJ software, Brunauer-Emmett-Teller (BET) (surface area quantachrome Nova 4200e instrument, Jogjakarta), fourier transform infrared (FTIR), atomic absorption spectrophotometer (AAS), scanning electron microscope (SEM), scanning electron microscopy-energy dispersive x-ray (SEM-EDS), and turbidimeter.

2.2 Extraction of Water Hyacinth Cellulose and Shrimp Shell Chitosan

Cellulose extraction was carried out based on the method [17]. 40 g water hyacinth powder was dissolved in 4% NaOH for 2 h at 70°C, then neutralized with distilled water and dried. The residue was dissolved with 3% H_2O_2 for 3 h at 70 ºC. Neutralization was carried out to pH 6 and dried for 3 h at 50 ºC. Chitosan extraction was carried out based on the method [18]. A 50 g dried shrimp shell powder was dissolved into 5% HCl for 2 h at 90 °C, then neutralized and dried for 3 h. The residue was dissolved into 3.5% NaOH for 1.5 h at 90 ºC, then neutralized and dried for 3 h. The residue was dissolved into 0.315% NaOCl for 1 h at 27 ºC. After that, it was dissolved into 50% NaOH for 2 h at 100 ºC. The residue was neutralized and dried for 6 h at 60 ºC. The resulting chitosan and cellulose were analyzed for typical functional groups using an FTIR instrument [19].

2.3 Shrimp Shell Nano-chitosan Synthesis

The synthesis of nano-chitosan refers to the previous method [15]. A 50 mL chitosan stock solution was prepared in 1% acetic acid with a concentration of 30 mg/L, added with distilled water to a volume of 500 mL, and homogenized for 2 h at 25°C. Tween 80 was added and homogenized as 0.1% for 2 h at 500 rpm and 100 mL of sodium tripolyphosphate (STPP) 0.1% was added drop by drop for 1 hour. Precipitation was carried out for 15 min at 15,000 rpm until a supernatant was obtained. The supernatant was dried using a dehydrator for 2 h at 70-80°C to produce nano-chitosan powder [20], and analyzed using SEM-EDS with gold coating.

2.4 Formulation of Water Hyacinth Cellulose Aerogel and Shrimp Shell Nano-chitosan

The preparation of aerogel followed the method [21], with modifications. Cellulose was dissolved in a mixture of NaOH (g), urea (g), and distilled water (mL) at a ratio of 7:12:81, and stirred for 1 hour at 50ºC. The aerogel formulations in this study were varied based on different ratios of cellulose to nano-chitosan. Nano-chitosan powder was then added and homogenized for 30 min. Subsequently, a 3% alginate solution was incorporated. The resulting gel precursor was molded into 1 cm^3 blocks and frozen for 24 h at -19ºC. The gel precursor was then immersed in a 3% $CaCl_2$ solution for 3 h, followed by soaking in 99% p.a. ethanol for 24 h. Finally, the gel was left at room temperature for 24 h and dried using a freeze dryer for 24 h at -40ºC

Table 1. Formula of water hyacinth cellulose aerogel and shrimp shell nano-chitosan

Treatment	Materials					
	Cellulose (g)	Nano-chitosan (g)	Urea (g)	NaoH (g)	Aquades (mL)	3% Alginate Solution (mL)
F1	2	1	7	12	81	100
F2	1	1	7	12	81	100
F3	1	2	7	12	81	100
K (-)	0	0	0	0	0	100

Note: Comparison of cellulose: nano-chitosan F1 (2:1), F2 (1:1), F3 (1:2)

2.5 Aerogel Precursor Characteristic

The gel content was measured by using 2.05 g of the gel precursor (Wo), which was wrapped in gauze and soaked in 20 mL of distilled water for 24 h. Afterward, the sample was dried for 2 h, and the final weight (Wt) was recorded. The gel content was calculated using the formula: Gel content (%) = $(W_t/W_o) \times 100\%$ [22]. The swelling ratio was determined by weighing 2.05 g of the gel precursor (Wo), soaking it in distilled water for 24 h, and then recording the final weight (Wt). The swelling ratio was calculated using the formula: Swelling ratio (%) = $(W_t/W_o) \times 100\%$ [22]. Viscosity was measured using a Brookfield viscometer (DV 1-Prime) with a spindle size of six at a speed of 60 rpm [23]. The results of the gel content test, swelling ratio, and viscosity were used as key parameters for determining the optimal aerogel formulation.

2.6 Characteristics Aerogel

The structural analysis of the aerogel was conducted in accordance with the method described by Farobie [24] (using Scanning Electron Microscopy (SEM) [24]. Parameters such as porosity, density, pore size, and surface area were analyzed following the procedure outlined [25] using the Brunauer-Emmett-Teller (BET) technique and the Quantachrome Nova 4200e surface area analyser [25]. Water absorption capacity was evaluated based on the methodology [26], wherein the aerogel was immersed in 10 mL of distilled water, and its weight was measured before (Wo) and after (Wt) 24 h of absorption. The water absorption capacity was calculated using the following formula. Following the characterization of the

optimal aerogel formulation, an application test was conducted best aerogel formula were continued with an application test.

$$\text{Water Absorption Capacity (\%)} = \frac{W_0 - W_t}{W_0} \times 100\% \qquad (1)$$

Description:
W_0 = Starting weight (g)
W_1 = Final weight (g)

The results of the characteristics of the best aerogel formula were continued with the application test.

2.7 Application Test of Aerogel

2.7.1 Turbidity Test

The turbidity test was carried out by soaking 2 g of F3 aerogel and alginate in a solution of water mixed with soil in a ratio of 1:30 with three replications. Turbidity was measured before and after the soaking process for 1 hour using a turbidimeter [27].

2.7.2 Heavy Metal Test

Heavy metal testing of the best aerogel formula refers to the method [28] with modifications. Metal Zn 0.434 g, Pb 0.212 g, and Cu 0.030 g were dissolved with distilled water and 10 mL of concentrated NHO_3 was added. Aerogel of 2 g per sample was added and homogenized for 24 h. The sample was heated to 20 mL, filtered, and diluted with distilled water until homogeneous. The samples were analyzed using an atomic absorption spectrophotometer (AAS) with wavelengths of 283.3 nm (Pb), 324.8 nm (Cu), and 213.9 nm (Zn) [29].

$$\text{Adsorption efficiency (\%)} = \frac{C_{initial} - C_{final}}{C_{final}} \times 100\% \qquad (2)$$

Description:
Initial C = Initial concentration of metal in solution (mg/L)
Final C = Final concentration of metal in solution (mg/L).

2.7.3 Total Microbial Test

Total microbial testing was conducted using the total plate count (TPC) method. The best aerogel formula and alginate as much as 2 g were soaked in NB solution with a ratio of 1:20 (b/v) for 24 h. Furthermore, the NB solution of each treatment was taken aseptically as much as 1 mL and diluted at the dilution level of 10-1-10-8. The 10-6-10-8 dilution was taken as two ose and inoculated into a petri dish containing NA media and incubated 24 h at 37 ºC. The growing colonies were counted using a colony counter. The results of bacterial growth were re-inoculated in a petri dish containing EMBA media as a selective medium for *E. coli* bacteria [30].

2.8 Data Analysis

Data were analyzed using one way ANOVA with 95% confidence interval. Each formula was tested with as many as three replicates. If the data analyzed were significantly different ($p<0.05$), then Duncan's further test was conducted.

3 Results and Discussions

3.1 Water Hyacinth Cellulose, Chitosan, and Shrimp Shell Nano-chitosan Yield

The S-EG extraction in this study produced a yield of 12.46%, almost the same as the research [31], which was 12.45%. This result was obtained due to shrinkage in water hyacinth during the delignification and bleaching process. This shrinkage is caused by breaking lignocellulose bonds in water hyacinth so that lignin and hemicellulose are degraded, and cellulose remains [10]. The yield of shrimp shell chitosan was obtained at 11.23%, close to the research results [12] of 12.46%. In addition, the NK-CU yield was 80%, close to the research results [32] of 80.67%. This is influenced by the high speed in the homogenization process between the ionic gelation material and the chitosan solution, resulting in stable nanoparticles and no agglomeration, which facilitates the drying process of nano-chitosan particles [32].

3.2 Micro Morphological Analysis

This outcome is influenced by the high-speed homogenization process between the ionic gelation agent and the chitosan solution, which leads to the formation of stable nanoparticles [32].

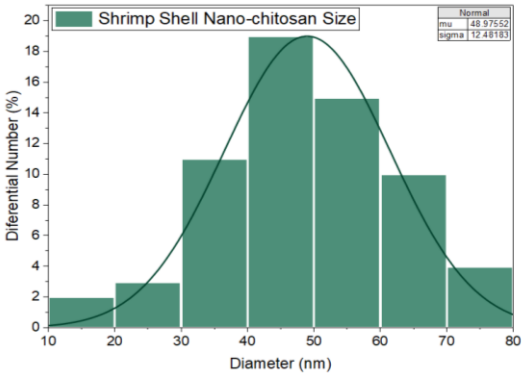

Fig. 1. Particle size of gold-coated nano-chitosan using SEM-EDS

The frequency of molecular collisions plays a significant role in determining the size of nano-chitosan particles. Increased collision intensity between solvent molecules and chitosan results in smaller particle sizes [33]. SEM-EDS analysis with a gold coating revealed an average nano-chitosan particle size of 48.97 nm (Fig. 1), which aligns with the standard nanoparticle size range of 10–1000 nm [34].

3.3 Functional Group Analysis of Water Hyacinth Cellulose and Shrimp Shell Chitosan

Cellulose contains characteristic functional groups such as -OH, -CH, and -CO [35]. These functional groups are present on the surface of aerogels, enabling them to chelate heavy metals [36]. The FTIR spectrum of cellulose exhibits peaks in the range of 3479–2889 cm^{-1} (Fig. 2), confirming the presence of cellulose. Similarly, chitosan is characterized by functional groups including -NH_2, -CH, and –OH [36]. The FTIR spectrum of chitosan shows peaks in the range of 3468–1101 cm^{-1}, providing evidence for the presence of chitosan.

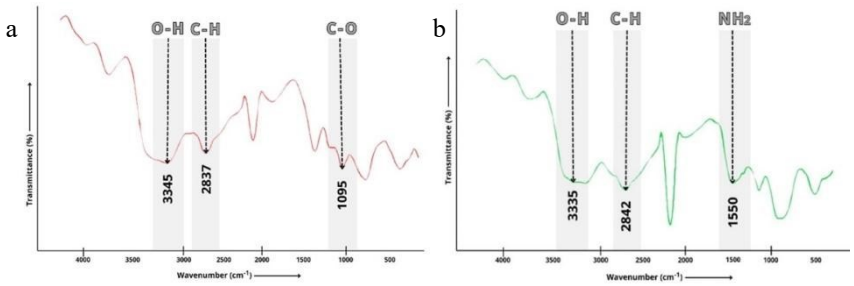

Fig. 2. FTIR spectrum of water hyacinth cellulose (a) and shrimp shell chitosan (b)

3.4 Aerogel Precursor Characteristic

Gel content testing indicates that the gel precursors F1 and F3 met the minimum reference value of 80%, as established [22]. The increase in cellulose as a composite reinforcement correlates with a higher gel content [37], further enhanced by the addition of $CaCl_2$. This occurs due to the formation of cross-links between the -OH groups in cellulose and the -NH_2 groups in nano-chitosan with $CaCl_2$. These cross-links increase the electrostatic interaction between anionic charges on the polymer chain and multivalent cations (Ca^{2+}), thereby reinforcing the ionic bonds between cellulose and nano-chitosan [38].

Swelling ratio analysis indicates that the highest swelling ratio is exhibited by the F3 gel precursor (Table 2), meeting the minimum standard of 75.83% [39]. The gel precursor demonstrates continuous water absorption, leading to uniform distribution of water throughout its network. This suggests that increasing the nano-chitosan ratio in the F3 gel precursor (1:2) enhances the formation of cavities, thereby increasing its water absorption capacity [40]. Conversely, the F1 gel precursor (2:1) exhibits the lowest swelling ratio, likely due to the higher polymer density, which impedes water absorption [41]. The increase in swelling ratio observed with the addition of chitosan is due to the high content of amine groups which are hydrophilic, thus increasing water absorption [42]. The hydroxyl group (-OH) present in chitosan can inhibit the formation of crosslinks between polymer chains leading to reduced crosslink density. This reduced crosslinking facilitates higher water absorption capacity in aerogel precursors [22].

Gel viscosity testing revealed that the F3 gel precursor exhibited the highest viscosity, falling within the standard range of 2000-4000 cPs [23]. The results indicate that an increase in nano-chitosan content correlates with an increase in viscosity. The incorporation of nano-chitosan enhances the physical properties of the gel by increasing the cross-linking density, thus reinforcing the gel structure [41]. Consequently, the combined results of gel content, swelling ratio, and viscosity tests indicate that the F3 formulation is the optimal choice.

Table 2. Characteristics of water hyacinth cellulose hydrogel and shrimp shell nano-chitosan

Parameter	Treatment			References
	F1(2:1)	F2 (1:1)	F3 (1:2)	
Gel Content (%)	84.88 ± 2.13^{a}	74.12 ± 1.76^{c}	80.16 ± 1.23^{b}	≤80 [28]
Swelling Ratio (%)	113.66 ± 0.84^{c}	119.19 ± 1.02^{b}	143.41 ± 0.84^{a}	<75.83 [32]
Viscosity (cPs)	1102 ± 67.04^{c}	1108 ± 27.74^{b}	3630 ± 39.53^{a}	2000-4000 [29]

Note: Different letters in the same row indicate significant differences ($p<0.05$).

3.5 Aerogel's Characteristic

3.5.1 FTIR Characterization of Aerogel

The Fourier Transform Infrared (FTIR) spectrum analysis of the aerogel was performed to confirm the presence of cellulose and chitosan components. Cellulose is characterized by the presence of typical functional groups such as OH, -CH, and –CO [35], while chitosan is identified by its -NH2, -CH, and -OH functional groups [43]. The FTIR spectrum reveals wavenumbers for the F1, F2, and F3 samples at 3318-2922 cm^{-1}, 3306-2923 cm^{-1}, and 3301-2934 cm^{-1}, respectively (Fig. 3) indicating the successful incorporation of cellulose and chitosan into the aerogel structure.

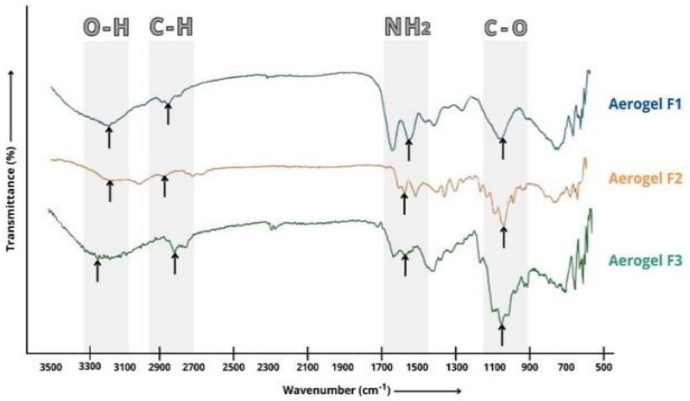

Fig. 3. FTIR spectrum of aerogels F1, F2, and F3

3.6 Water Absorption Capacity of Aerogel

The test results demonstrated that the F3 aerogel exhibited the highest water absorption capacity. The increased nano-chitosan ratio enhances water absorption due to the presence of hydrophilic hydroxyl and amine groups, which interact with water molecules through hydrogen bonding. Furthermore, nano-chitosan creates more pores compared to cellulose, further promoting water absorption in the F3 aerogel [22].

The results of testing the absorption capacity of aerogel (cellulose:nano-chitosan) showed significant differences between formulas (Fig. 4). Formula F1 (2:1), with a higher cellulose content, has the lowest water absorption capacity because cellulose has fewer hydrophilic groups and pores, so its interaction with air through hydrogen bonds is limited [44]. In Formula F2 (1:1), the absorption capacity increases due to the balanced ratio between cellulose and nano-chitosan, which increases the number of hydroxyl groups and hydrophilic amines and increases the number of pores, increasing interaction with water. The formula with the highest water absorption capacity is formula F3 (1:2), where the nano-chitosan ratio is higher than cellulose. Nano-chitosan is known to have more hydrophilic groups, especially hydroxyl and amine groups, which enable stronger interactions with water molecules through hydrogen bonds [22]. In addition, nano-chitosan also contributes to the formation of a wider porous structure compared to cellulose, thereby facilitating greater water absorption. The presence of more pores increases the internal surface area of the aerogel, allowing more water to be absorbed.

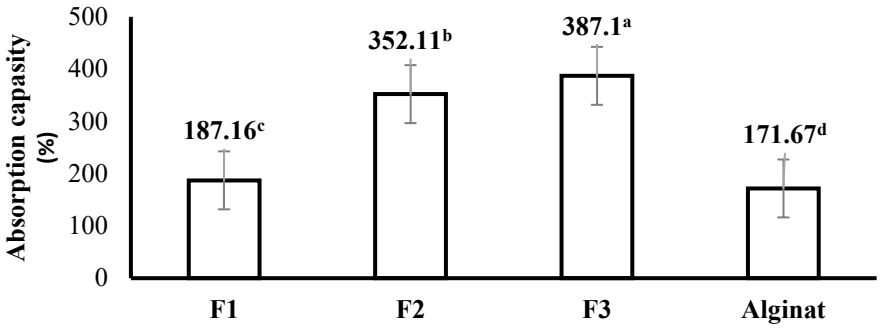

Fig. 4. Results of water absorption capacity of aerogel
Note: Different letters in the same graphic indicate significant differences ($p<0.05$)

3.7 Morphological Structure of Aerogel

SEM analysis showed structural differences in F1, F2, and F3 aerogels (Fig. 5). F1 has a dense structure with coarse fibers and tight pores, F2 shows fine fibers with non-uniform pores, while F3 has fine fibers with tight and uniform pores. Aerogel F3 has an ideal morphology as a good adsorbent biomaterial. This is supported by significant hardening due to compaction of the porous structure in good aerogels [45].

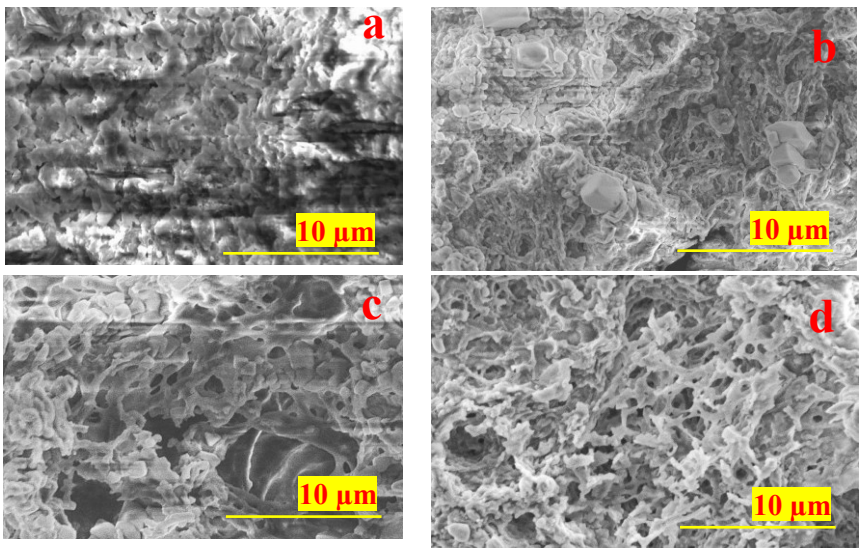

Fig. 5. SEM aerogel magnification 5000x: a) Alginate, b) F1(2:1), c) F2 (1:1), d) F3 (1:2).

3.8 Aerogel Adsorbent Characterization Results

The Brunauer-Emmett-Teller (BET) analysis of the F3 aerogel (Table 3**)** confirms its suitability as a highly effective porous material, as its characteristic values fall within the standard range typically observed for aerogels

Table 3. Results of Porosity, density, pore size, and surface area of aerogel

Results	F3	Reference
Density (g/cm^3)	0.007	0.003-0.5 [46]
Surface Area (m^2/g)	243.5	100-1600 [46]
Pore Size (nm)	6.61	2-50 [47]
Porosity (%)	97.0	80-99.8 [48]

The F3 aerogel exhibits high porosity and low density, indicating that increasing the nano-chitosan ratio enhances porosity, whereas increasing the cellulose ratio leads to a denser structure with reduced porosity [48]. The porosity of aerogels is directly correlated with their water absorption capacity [49], as demonstrated by tests showing that F3 achieves the highest absorption capacity, while F1 exhibits the lowest. Additionally, porosity regulates water flow and influences the interaction of functional groups, which in turn improves pollutant removal efficiency [50]. According to the findings of Horvat [47], the F3 aerogel features a mesoporous structure.

3.9 Aerogel Application in Heavy Metal Removal and Bacteria Filtration

3.9.1 Aerogel's Turbidity

Turbidity testing was conducted to determine the ability of the aerogel to reduce water turbidity levels. The test results showed that the highest reduction was achieved with F3 cellulose aerogel (1:2). F3 aerogel was more effective in reducing water turbidity than other formulations. This is due to the presence of hydroxyl groups (-OH) in nano-chitosan and cellulose, which are hydrophilic, enabling the aerogel to absorb turbid water effectively. In addition, chitosan has strong coagulation properties, helping to bind the fine particles causing turbidity and making the flocculation process more effective. F3 aerogel demonstrates a better synergistic effect with a higher combination of cellulose and nano-chitosan, enhancing flocculation and adsorption capacity, which is essential for binding and absorbing dirt particles in water more efficiently [51]. Research by Wang [52] supports this finding that aerogel as a coagulant has practical flocculation ability in reducing water turbidity through adsorption properties. Aerogel F3 is more effective in reducing water turbidity by 38.19 ± 6.43 compared to the study conducted by [53], which achieved a reduction of 15.02 ± 3.44. This is attributed to a synergistic effect between the two materials in aerogel F3. Cellulose serves as a component that provides a wide porous structure, while nanochitosan acts as a flocculating agent that enhances the ability of the aerogel to bind small particles causing turbidity.

Table 4. Results of turbidity of aerogel samples

Treatment	Turbidity reduction (%)
Aerogel (F3)	38.19 ± 6.43^a
Alginate (-)	11.60 ± 0.32^b
Control solution	11.23 ± 0.00^b

Description: Different letters in the same column indicate significant differences ($p<0.05$)

3.9.2 Microbial Analysis for Selected Aerogel

Total microbial test is carried out using the total plate count (TPC) method. TPC is performed to indicate the number of microorganisms in a sample. TPC testing shows that the growth rate of E. coli bacteria is high in the control and alginate, while in F3 aerogel, there is a decrease (Table 7). The decrease in *E. coli* indicates that the aerogel can filter and reduce *E. coli* bacteria. According to Pan [54], aerogel can reduce the total microbes with nano-chitosan, which provides antibacterial activity against *E. coli*. The presence of nano chitosan in Aerogel F3 can inhibit bacterial growth by 30% (Table 5). This is similar to the research of Magani [55] which showed that nano chitosan can inhibit E. coli bacteria by up to 40%. Therefore, nano chitosan is bacteriostatic, which successfully suppresses or prevents the growth of *E. coli* bacteria (Fig. 6).

Table 5. Calculation of the number of colonies of the F3 aerogel sample

Treatment	Total Cells (CFU/mL)
Aerogel (F3)	6.3×10^7
Control - (alginate)	34×10^7
Control + (*E. coli*)	9.0×10^7

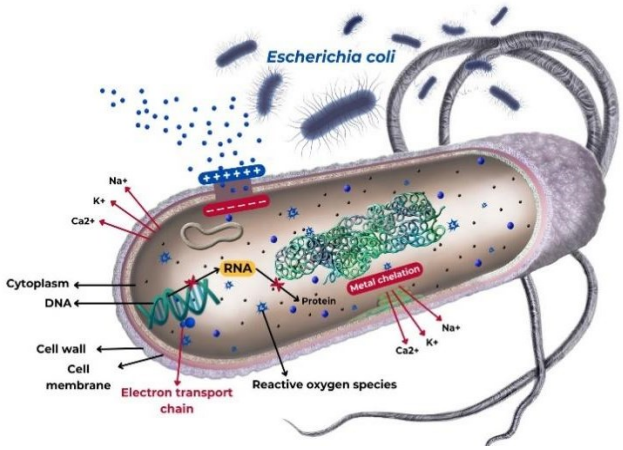

Fig. 6. *E. coli* Filtration Mechanism (inhibits growth)

The antibacterial mechanism of nano-chitosan operates through electrostatic interactions between the positively charged nano-chitosan and negatively charged bacterial cell membranes, resulting in the disruption of the membrane structure. This disruption compromises the stability of the cell wall and increases membrane permeability, allowing harmful external substances to penetrate the cell. The increased permeability causes leakage of intracellular ions, such as K+ and Na+, resulting in osmotic imbalance and disruption of bacterial homeostasis. Furthermore, nano-chitosan inhibits the electron transport chain, reducing the essential energy production required for bacterial survival. Nano-chitosan also induces the formation of reactive oxygen species (ROS), which generate oxidative stress and cause damage to bacterial DNA, impairing replication and transcription processes. Additionally, nano-chitosan has the ability to chelate essential metal ions such as Fe^{2+}, Mg^{2+}, and Zn^{2+}, further disrupting bacterial physiological stability. The cumulative effects of these disruptions act synergistically, ultimately leading to the death of the bacterial cells [16]. Another report of biopolymer material that can be used as a composite or precursor for

aerogel is pectin. Pectin is a valuable candidate for aerogel use due to its antimicrobial properties. According to Ciriminna [56], pectin can act as an antimicrobial through several main mechanisms, mainly due to its ability to bind and destroy the outer membrane of microbes.

3.9.3 Heavy Metal Content of Selected Aerogel

Heavy metal testing of the F3 aerogel was conducted following the method outlined by [28], with modifications. Zn (0.434 g), Pb (0.212 g), and Cu (0.030 g) metals were dissolved in distilled water, followed by the addition of 10 mL of concentrated HNO_3. A total of 2 g of aerogel per sample was added and homogenized for 24 h. The sample was then heated until the volume was reduced to 20 mL, filtered, and further diluted with distilled water until a homogeneous solution was obtained. The samples were analyzed using an Atomic Absorption Spectrophotometer (AAS) at wavelengths of 283.3 nm for Pb, 324.8 nm for Cu, and 213.9 nm for Zn [57].

Table 6. Heavy metal test results on F3 aerogel sample.

Metal (mg/L)	Sample			F3 Adsorption Efficiency (%)	Alginate Adsorption Efficiency (%)
	Aerogel F3	Alginate	Control (-)		
Copper (Cu)	0.055 ± 0.005	12.276 ± 0.025	12.920	99.57[a]	4.98[a]
Zinc (Zn)	0.702 ± 0.002	6.167 ± 0.0064	6.207	88.40[b]	0.64[c]
Lead (Pb)	90.900 ± 0.100	97.105 ± 0.005	98.089	7.33[c]	1.00[b]

Description: Different letters in the same row indicate significant differences ($p<0.05$).

Heavy metal testing was conducted to assess the adsorption efficiency of the F3 aerogel for different heavy metals. The results indicate that the F3 aerogel exhibits higher adsorption efficiency for Cu^{2+} and Zn^{2+} ions compared to Pb^{2+} ions (Table 6). This difference in adsorption efficiency can be attributed to the larger ionic radius of Pb^{2+}, its weaker chemical affinity with the $-NH_2$ and -OH functional groups, and increased ion competition favoring Cu^{2+} and Zn^{2+}. Additionally, at neutral pH (7), the adsorption of Pb^{2+} by the aerogel decreases due to minimal equilibrium shifts, weakening its interaction with the $-COO^-$ groups [56].

The porous structure of the aerogel, combined with the chemical interactions between its components and metal ions, along with the alkaline conditions provided by NaOH, enhances its adsorption affinity. The amine ($-NH_2$) and hydroxyl (-OH) groups present in nano-chitosan serve as active sites for metal ion binding [42]. These functional groups exhibit high reactivity, allowing nano-chitosan to act as an electron donor. This mechanism involves the NH_2 ligand donating a pair of electrons to the metal ion, forming a coordinate covalent bond, thereby enabling nano-chitosan to chelate heavy metal ions [58].

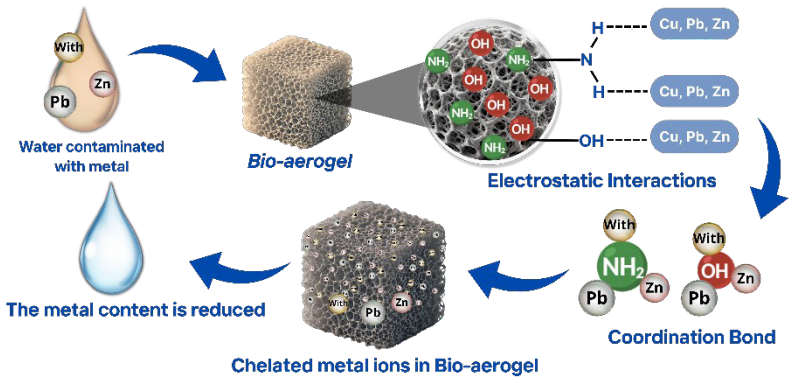

Fig. 7. Mechanism of Heavy Metal Adsorption with generated aerogel

The schematic process for heavy metal adsorption by bio-aerogels, begins with heavy metal contaminants in solution, where bio-aerogels containing amine (-NH_2) and hydroxyl (-OH) groups serve as active sites for metal ion binding [59], was re-illustrated in Fig 7**.** The contaminants are absorbed onto the porous surface of the aerogel through various adsorption mechanisms. The incorporation of cellulose and nano-chitosan increases the adsorption capacity by enhancing the surface electronegativity of the adsorbent. Electrostatic interactions between the charged molecules further facilitate the retention of metal ions, making it more difficult for them to detach from the aerogel's pores. Additionally, ion exchange plays a crucial role, where ions from the adsorbent surface are released in equal amounts to those absorbed. For example, Cu^{2+} forms coordination bonds with nitrogen or oxygen atoms from the -NH_2 and -OH groups, while similar coordination interactions occur between metal ions and oxygen atoms during the removal of Pb^{2+}, Cu^{2+}, and Zn^{2+} by cellulose- and nano-chitosan-based bio-aerogels [59].

4 Conclusions

This study successfully developed aerogels from water hyacinth cellulose (S-EG) and shrimp shell nano-chitosan (NK-CU), with the optimal formulation being Aerogel F3, utilizing a cellulose-to-nano-chitosan ratio of 1:2. Aerogel F3 exhibited superior performance in multiple key areas, achieving high heavy metal adsorption efficiencies of 99.50% for Cu^{2+}, 88.86% for Zn^{2+}, and 7.33% for Pb^{2+}. In addition, Aerogel F3 demonstrated effective bacterial filtration, reducing *Escherichia coli* by 30%, and achieved a 38.19% reduction in water turbidity. These results highlight the potential of Aerogel F3 as a promising material for environmental remediation, particularly in heavy metal removal and microbial contamination reduction in polluted water. However, further optimization may be needed to enhance its adsorption capacity for lead and improve its antibacterial efficacy for broader practical applications.

The authors gratefully acknowledge the Ministry of Education, Culture, Research, and Technology, Student Creativity Program (PKM), IPB University, Indonesia, for funding the Student Creativity Program (Grant Number for PKM Funding Scheme 2024: 2546/E2/DT.01.00/2024). Our sincere thanks are extended to the Directorate of Student Affairs, IPB University, for their support in facilitating and partially funding this research. We also thank Prof. Uju and the IPB University JSPS Team, as well as Dr. Novitri Hastuti from the Research Center for Biomass and Bioproducts, National Research and Innovation Agency, Indonesia, for kindly providing the cellulose standard used in the experiment.

References

1. I.K. Sari, L.L. Montarcih, D. Priyantoro, Analisa ketersediaan dan kebutuhan air pada DAS Sampean. Jurnal Teknik Pengairan. **2**, 1 (2011).
2. Badan Pusat Statistik. Statistik air bersih 2018-2022. (Badan Pusat Statistik, Jakarta, 2023)
3. M. Darmasetiawan, Pengolahan air minum satuan operasi (PT. Kimshafi Alung Cipta, Bekasi, (2024)
4. Triyanto, Analisa instalasi pengolahan air minum PDAM Kota Gorontalo. Jurnal Peradaban Sains, Rekayasa dan Teknologi. **4**, 1 (2019). https://doi.org/10.37971/radial.v4i1.118
5. B. Yohannes, S.W. Utamo, A. Haruki, Kajian kualitas air sungai dan upaya pengendalian pencemaran air (studi di Sungai Krukut, Jakarta Selatan). Indonesian Journal of Environmental Education and Management. **4**, 2 (2019). https://doi.org/10.21009/IJEEM.042.05
6. R. Rahmi, S. Sajidah, Pemanfaatan adsorben alami (biosorben) untuk mengurangi kadar timbal (Pb) dalam limbah cair. Prosiding Seminar Nasional Biotik 2017, Banda Aceh, Indonesia, Oktober 3-7, Oktober 3-7 (2018). http://dx.doi.org/10.22373/pbio.v5i1.2162
7. Y.H. Zhu, Q. Zhang, G.T. Sun, C.Z. Chen, M.Q. Zhu, X.H. Huang, The synthesis of tannin-based graphene aerogel by hydrothermal treatment for removal of heavy metal ions. Industrial Crops and Products. **176**, 1 (2022). http://dx.doi.org/10.1016/j.indcrop.2021.114304
8. J.K. Parker, S. Lignou, K. Shankland, P. Kurwie, H.D. Griffiths, D.A. Baines, Development of a zeolite filter for removing polycyclic aromatic hydrocarbons (PAHs) from smoke and smoked ingredients while retaining the smoky flavour. Journal of Agricultural and Food Chemistry. **66**, 10 (2017). https://doi.org/10.1021/acs.jafc.6b05399
9. A.C. Boccia, M. Neagu, A. Pulvirenti, Bio-based aerogels for the removal of heavy metal ions and oils from water: Novel solutions for environmental remediation. Gels. **10**, 1 (2023). https://doi.org/10.3390/gels10010032
10. J.H. Pratama, R.L. Rohmah, A. Amalia and T.E. Saraswati, Isolasi mikroselulosa dari limbah eceng gondok (*Eichornia crassipes*) dengan metode bleaching-alkalinasi. ALCHEMY. **15**, 2 (2019). https://doi.org/10.20961/alchemy.15.2.30862.239-250
11. T. Poernama, E. Pebriansyah, A.L. Arifin, R. Yusuf, Ubah gulma menjadi emas: Studi kasus pengolahan eceng gondok menjadi humus aktif dan enzimatik di Waduk Jatiluhur Purwakarta. E-BISMA. **4**, 1 (2023). http://dx.doi.org/10.37631/ebisma.v4i1.869
12. S.L. Ihsani, C.R. Widyastuti, Sintesis biokoagulan berbasis kitosan dari kulit udang untuk pengolahan air sungai yang tercemar limbah industri jamu dengan kandungan padatan tersuspensi tinggi. Jurnal Bahan Alam Terbarukan. **3,** 2 (2014). https://doi.org/10.15294/jbat.v3i2.3700
13. Kementerian Kelautan dan Perikanan. Rilis Data Kelautan dan Perikanan Triwulan Tahun 2022, (Pusat Data, Statistik, dan Informasi Sekretariat Jenderal Kementrian Kelautan dan Perikanan, Jakarta, 2022)
14. M. Chandrasekaran, K.D. Kim, S.C. Chun, Antibacterial activity of chitosan nanoparticles: A review. Processes. **8**, 1 (2020). https://doi.org/10.3390/pr8091173
15. S.D. Hardiningtyas, D.F. Bahri, P. Suptijah, Aktivitas antimikroba nanokitosan cangkang udang sebagai sediaan pembersih tangan. Journal of Marine and Coastal Science. **11**, 1 (2022). https://doi.org/10.20473/jmcs.v11i1.33821
16. K.T. Mai, P. Wang, G. Ma, Promising cellulose-based aerogel composites: Preparation methods and advanced applications. Composites Part B: Engineering. **281**, 111559 (2024). https://doi.org/10.1016/j.compositesb.2024.111559
17. E. Kusumawati, H. Haryadi, Ekstraksi dan karakterisasi serat selulosa dari tanaman

eceng gondok (*Eichornia crassipes*). Fluida. **14**, 1 (2021). https://doi.org/10.35313/fluida.v14i1.3452
18. A.R. Kusmiati, N. Nurhayati, Pemanfaatan kitosan dari cangkang udang sebagai adsorben ion logam berat Pb pada limbah praktikum kimia farmasi. IJIL. **3**, 1 (2020). https://doi.org/10.22146/ijl.v3i1.60789
19. L. Trisnawati, D. Kurniawan, F.U. Ajri, F. Sinurat, Optimalisasi produksi oligomer dari kitosan hasil ekstraksi kepala udang menggunakan aplikasi iridiasi gamma, Jurnal Ilmiah Sain dan Teknologi. **2**, 8 (2024). https://doi.org/10.572349/scientica.v2i8.2262
20. P.L. Curone, E. Testi, M. Macías, S. Tazzari, J.P. Facchini, C.J. Williams, Clarke, Radio multiwavelength analysis of the compact disk CX Tau: Presence of strong free-free variability or anomalous microwave emission. Astronomy and Astrophysics. **677**, 23 (2023). https://doi.org/10.1051/0004-6361/202347042
21. H. Peng, J. Wu, Y. Wang, H. Wang, Z. Liu, Y. Shi, X. Guo, A facile approach for preparation of underwater superoleophobicity cellulose/chitosan composite aerogel for oil/water separation. Applied Physics. **122**, 1 (2016).
22. U.L. Fadiana, Haryanto, Pengaruh kitosan terhadap karakterisasi hidrogel film pva untuk aplikasi pembalut luka. Techno. **22**, 2 (2021). http://dx.doi.org/10.30595/techno.v22i2.11593
23. R. Setiawan, C.D.P. Masrijal, O. Hermansyah, S. Rahmawati, R.I.P. Sari, A.N. Cahyani, Formulasi, evaluasi, dan uji stabilitas fisik sediaan gel antioksidan ekstrak tali putri (*Cassytha filiformis* L). Bencoolen Journal of Pharmacy. **3,** 1 (2023). https://doi.org/10.33369/bjp.v3i1.27649
24. O. Farobie, A. Amrullah, A. Bayu, N. Syaftika, L.A. Anis, E. Hartulistiyoso, In-depth study of bio-oil and biochar production from macroalgae Sargassum sp. via slow pyrolysis. RSC Advances. **12**, 16 (2022). https://doi.org/10.1039/D2RA00702A
25. M. Tripathi, A. Bhatnagar, N.M. Mubarak, J.N. Sahu, P. Ganesan, RSM optimization of microwave pyrolysis parameters to produce OPS char with high yield and large BET surface area. Fuel. **277**, 1 (2020). https://doi.org/10.1016/j.fuel.2020.118184
26. L. Huang, W. Lee, Y. Chen, Bio-based hydrogel and aerogel composites prepared by combining cellulose solutions and waterborne polyurethane. Polymers. **14**, 1 (2022). https://doi.org/10.3390/polym14010204
27. R. Andrianto, I.Y. Perwira, I.K.W. Negara, Analisa kualitas air di sungai Pelus, Purbalingga, Jawa Tengah. Current Trends in Aquatic Science. **4**, 1 (2021)
28. M.A.R. Pambudi, S. Suprapto, Penentuan kadar tembaga (Cu) dalam sampel batuan mineral. Jurnal Sains dan Seni ITS. **7**, 2 (2019). http://dx.doi.org/10.12962/j23373520.v7i2.30088
29. N. Rosita, Analisis logam berat Pb, Fe, dan Mn air tanah sekitar tempat pembuangan akhir sampah Tanggerang. ALOTROP. **7**, 1 (2023). https://doi.org/10.33369/alo.v7i1.23239
30. A. Lestrari, Rukmini, T.H.R. Sunarti, N.R. Amelia, A. Fatiqin. Analisis total Coliform pada perairan sungai di kabupaten Musi Rwas Utawa Sumatera Selatan. Journal Biotropical Research and Nature Technology. **1**, 1 (2022). https://doi.org/10.36873/borneo.v1i1.7342
31. L. Setyaningsih, E. Satria, H. Khoironi, M. Dwisari, G. Setyowati, N. Rachmawati, J. Anggraeni, Cellulose extracted from water hyacinth and the application in hydrogel. Materials Science and Engineering. **673**, 1 (2019). http://dx.doi.org/10.1088/1757-899X/673/1/012017
32. L.M.H. Nadia, P. Suptijah, B. Ibrahim, Produksi dan karakterisasi nano kitosan dari cangkang udang windu dengan metode gelasi ionik. Jurnal Pengolahan Hasil Perikanan Indonesia. **17**, 2 (2014)
33. S.R. Guge, A. Lukum, W.R. Kunusa, Pembuatan nano kitosan menggunakan metode

gelasi ionik. Jamb.J.Chem. **6**, 1 (2024)
34. N. Noval, S. Malahayati, Teknologi Penghantaran Obat Terkendali (UI Press, Jakarta, 2021).
35. N.R. Nurjannah, T. Sudiarti, L. Rahmidar, Sintesis dan karakterisasi selulosa termetilasi sebagai biokomposit hidrogel. Jurnal Ilmu Kimia dan Terapan. **7**, 1 (2020). https://doi.org/10.15575/ak.v7i1.6490
36. M.C. Djunaidi, Pengenalan metode adsorpsi logam Fe (III) menggunakan selulosa dan selulosa asetat dari serbuk gergaji kayu kepada siswa SMA Al-Azhar 14 Semarang. Pengabdian Masyarakat UNDIP. **1**, 1 (2020)
37. S. Brethauer, R.L. Shahab, M.H. Studer, Impacts of biofilms on the conversion of cellulose. Applied Microbiology and Biotecgnology. **104**, 2 (2020). https://doi.org/10.1007/s00253-020-10595-y
38. C.F.N. Nan, N. Zainuddin, M. Ahmad, Preparation and swelling study of CMC hydrogel as potential superabsorbent. Pertanika Journals Science and Technology. **21**, 1 (2019)
39. B. Pratiwi, S. Setiasih, S. Handayani, S. Hudiyono, Dissolution study of bromelain resulting from partial purification of pineapple stem (*Ananas comosus* [L.] *Merr*) encapsulated in chitosan-guar gum and its activity as an antipelet. AIP Advances. **2243**, (2020). https://doi.org/10.1063/5.0001347
40. D.Y. Rahayuningdyah, D. Lyrawati, F. Widodo, O.E. Puspita, Pengembangan formula hidrogel balutan luka menggunakan kombinasi polimer galaktomanan dan PVP. Pharmaceutical Journal of Indonesia. **5**, 2 (2020). http://doi.org/10.21776/ub.pji.2020.005.02.8
41. P.T. Anindyajati, P.S. Lastianny, F. Yogianti, K. Murdiastuti, Effect of collagen-chitosan hydrogel formula combined with platelet-rich plasma (A study pf pH, viscosity, and swelling test). Majalah Kedokteran Gigi Indonesia. **6**, 3 (2020). https://doi.org/10.22146/majkedgiind.44391
42. K. Zhang, W. Feng, C. Jin, Protocol efficiently measuring the swelling rate of hydrogels. PubMed Central. **19**, 7 (2019). https://doi.org/10.1016/j.mex.2019.100779
43. A. Romero-Montero, J. Valencia-Bermudez, A.S. Rosas-Melendez, I. Nufiez-Tapia, M.P. Pifia-Barba, G. Leyva-Gomez, L.M. Del, Recent advances in nanocellulose aerogels for efficient heavy metal and dye removal. Gels. **9**, 5 (2023). https://doi.org/10.3390/gels9050416
44. Chung-Yi Wu, Kuan-Ju Tu, Jin-Pei Deng, Yu-Shiu Lo, Chien-Hou Wu. Markedly Enhanced Surface Hydroxyl Groups of TiO2 Nanoparticles with Superior Water-Dispersibility for Photocatalysis. **10**, 5 (2017). https://doi.org/10.3390/ma10050566
45. D. Wang, H. Yu, X. Fan, J. Gu, S. Ye, J. Yao, Q. Ni, High aspect ratio carboxylated cellulose nanofibers cross-linked to robust aerogels for superabsorption-flocculants: paving way from nanoscale to macroscale. ACS Applied Materials and Interfaces. **10**, 24 (2018). https://doi.org/10.1021/acsami.8b04211
46. H. Maleki, Recent advances in aerogels for environmental remediation applications: A review. Chemical Engineering Journal. **300**, 1 (2016). https://doi.org/10.1016/j.cej.2016.04.098
47. G. Horvat, M. Pantic, Z. Knez, Z. Novak, A brief evaluation of pore structure determination for bioaerogels. Gels. **8**, 7 (2022). https://doi.org/10.3390/gels8070438
48. L. Nguyen Tan, N.C. Nguyen Thi, A.M.H. Trinh, N.H.N. Do, K.A. Le, P.K. Le, Eco-friendly synthesis of durable aerogel composites from chitosan and pineapple leaf-based cellulose for Cr(VI) removal. Separation and Purification Technology. **304**,122415 (2023). https://doi.org/10.1016/j.seppur.2022.122415
49. S. Rizal, E.B. Yahya, H.P.S.A. Khalil, C.K. Abdullah, M. Marwan, I. Ikramullah, U. Muksin, Preparation and characterization of nanocellulose/chitosan aerogel scaffolds

using chemical-free approach. Gels. **7**, 4 (2021). https://doi.org/10.3390/gels7040246
50. J. Paul, S.S. Ahankari, Nanocellulose-based aerogels for water purification: A review. Journal Carbohydrate Polymers. **309**, 120677 (2023). https://doi.org/10.1016/j.carbpol.2023.120677
51. E. Lichtfouse, N. Morin-Crini, M. Fourmentin, H. Zemmouri, I.O. do Carmo Nascimento, L.M Queiroz, G. Crini, Chitosan for direct bioflocculation of wastewater. Environmental Chemistry Letters. **7**, 4 (2019)
52. Z. Wang, R. Huang, Y. Zhang, C. Jia, C. Zhao, W. Chen, Y. Xue, Fabrication and characterization of cellulose nanofiber aerogels prepared visa two different drying techniques. Polymers. **12**, 2583 (2020). https://doi.org/10.3390/polym12112583
53. A, Pirozzi, E. Rincón, E. Espinosa, F. Donsì, L. Serrano. Nanostructured Cellulose-Based Aerogels: Influence of Chemical/Mechanical Cascade Processes on Quality Index for Benchmarking Dye Pollutant Adsorbents in Wastewater Treatment. Gels. **9**, 23 (2023). https://doi.org/10.3390/gels9120958
54. J. Pan, Y. Li, K. Chen, Y. Zhang, H. Zhang, Enhanced physical and antimicrobial properties of alginate/chitosan composite aerogels based on electrostatic interactions and noncovalent crosslinking. Carbohydrate Polymers. **266**, 3 (2021). https://doi.org/10.1016/j.carbpol.2021.118102
55. Magani, A. K., Tallei, T. E., Kolondam, B. J. Uji antibakteri nanopartikel kitosan terhadap pertumbuhan bakteri *Staphylococcus aureus* dan *Escherichia coli*. *Jurnal Bios Logos*. **10**, 1 (2020). https://doi.org/10.35799/jbl.10.1.2020.27978
56. Ciriminna, R., Fidalgo, A., Meneguzzo, F., Presentato, A., Scurria, A., Nuzzo, D., Alduina, R., Ilharco, L.M. and Pagliaro, M. Pectin: A long-neglected broad-spectrum antibacterial. *ChemMedChem*. **15**, 23 (2020). https://doi.org/10.1002/cmdc.202000518
57. S.J. Tangio, Adsorpsi logam timbal (Pb) dengan menggunakan biomassa enceng gondok (*Eichhornia crassipes*). Jurnal Entropi. **8**, 1 (2013). https://doi.org/10.37905/je.v8i1.1158
58. E. Susilowati, F.W. Mahatmanti, Haryani, Sintesis kitosan-silika bead sebagai pengadsorpsi ion logam Pb (II) pada limbah cair batik. Indonesian Journal of Chemical Science. **7**, 2 (2018). https://doi.org/10.15294/ijcs.v8i3.28725
59. A. Ahmad, M.A. Kamarudin, H.P.S.A. Khalil, E.B. Yahya, S. Muhammad, S. Rizal, M.I. Ahmad, I. Surya, Recent advances in nanocellulose aerogels for efficient heavy metal and dye removal. Gels. **9**, 416 (2023). https://doi.org/10.3390/gels9050416